Advanced MEMS-based nanomechanical testing: beyond stress and strain measurements

Sanjit Bhowmick, Horacio Espinosa, Katherine Jungjohann, Thomas Pardoen, Olivier Pierron*

The field of in-situ nanomechanics is greatly benefiting from microelectromechanical system (MEMS) technology and integrated microscale testing machines to measure a wide range of mechanical properties at nanometer scales while characterizing the damage or microstructure evolution in electron microscopes. This review focuses on the latest advances in MEMS-based nanomechanical testing techniques that go beyond stress and strain measurements under typical monotonic loadings. Specifically, the recent sophistications in MEMS testing machines now enable probing key mechanical properties of nanomaterials related to fracture, fatigue and wear. In addition, the tensile properties can be measured without instabilities or at high strain rates, and signature parameters such as activation volume can be obtained. Opportunities for environmental in-situ nanomechanics enabled by MEMS technology are also discussed.

Keywords: microelectro-mechanical (MEMS); transmission electron microscopy (TEM); fatigue; fracture; tribology; strength

Introduction

A growing number of in-situ electron microscopy nanomechanics investigations now rely on microelectromechanical systems (MEMS), either from instrumented, active MEMS devices, arrays of passive MEMS structures, or a passive “push-to-pull” PTP MEMS combined with a nanoindentation TEM holder.[1-9] These MEMS setups are ideal experimental platforms to simultaneously quantify mechanical properties and to characterize microstructure evolution at the nanometer scale, and can be supplemented and enriched with atomistic models to provide thorough understanding of defect mechanics.[10-13] So far, most of these studies have focused on elastic and plastic deformation under simple monotonic loadings. This article provides an overview of current efforts to perform in-situ advanced nanomechanical tests using integrated micro/nanofabrication, such as fracture, fatigue, and wear. With these setups, a thorough nanoscale understanding of defects mechanics under complex loading modes (e.g., cyclic, high strain rates, multiaxial), highly localized regions (i.e., shear instabilities crack tip, sample surface), and various reactive environments is now within reach.

In-Situ Tensile Tests

In-situ electron microscopy mechanical and electro-mechanical testing of materials, based on MEMS devices such as the one shown in Fig. 1(a), has been a very powerful approach to unambiguously establish *structure-property* relationships in low dimensional metallic and semiconducting materials.[2, 7] By integrating micro-scale electronic actuation (with nm resolution) and load sensing (with nN resolution), simultaneous acquisition of high-resolution images of the atomic structure of tested specimens was achieved. This enabled *direct* imaging of deformation and failure processes with unprecedented resolution.[14] For instance, the first direct correlation between failure stress and number of failed shells in multi-walled carbon nanotubes was obtained, which resolved literature discrepancies between theoretical quantum mechanical predictions and experimental measurements of Young's modulus and strength.[15] Inter-shell cross-linking effects, as a function of electron radiation dose, were also revealed.[14, 15]

By incorporating feedback control schemes in the MEMS devices both load and displacement control experiments can be performed. The displacement control tensile testing capability is particularly relevant to non-monotonic loading, fracture, and adhesion tests. Indeed, in all these instances there is a sudden release of elastic energy stored in the system, which requires stabilization through a feedback controller. To achieve a true displacement-controlled test in the MEMS shown in Fig. 1(a), an electrostatic actuator is implemented within a feedback loop. The voltage output from the load sensor is compared to a reference, with the difference (error) fed to a controller, which sends a voltage to the electrostatic actuator.[16] The voltage in the electrostatic actuator is then transformed to a force exerted on the load sensor keeping it quasi-stationary, see Fig. 1(a). The elongation and strain of the specimen are calculated from the applied voltage in the thermal actuator using a pre-calibrated voltage-displacement table. For simultaneous HRTEM imaging, the MEMS is mounted in a customized TEM sample holder.[17] An example of such testing is the non-monotonic testing of silver penta-twinned metallic nanowires in which direct observation of dislocation nucleation and identification of a recoverable plasticity mechanism, arising from dislocation-surface interactions, became possible[11] (see Fig. 1(b) and (c)). Examination of stress-strain curves obtained from nanowires of various diameters, revealed not only a size dependent yield stress but also an unusually strong Bauschinger effect,[11] Fig. 1 (d). Likewise, by exploiting the testing stability afforded by feedback-control, the mechanical reliability of single crystal silver nanowire-based systems was ascertained by identifying time-dependent stress-assisted atomic diffusion mechanisms, over several hours, leading to necking instabilities.[13] Remarkably, such non-monotonic deformation process is particularly relevant to emerging applications using transparent electrodes based on silver nanowire networks, such as flexible electronic sensors, solar cells, and touch screens.[18]

Characterization of thin films and low dimensional materials, as a function of strain rate, is another tensile testing mode of interest that goes beyond typical stress and strain measurements. In this regards, the low mass of microsystems combined with electronic actuation and sensing enables the exploration of rate effects.[12, 19] By employing such testing capability, bi-crystalline silver nanowires were tested in tension under a range of strain rates. Interestingly, a brittle to ductile transition was revealed at a strain rate of ~1/s (Fig. 2(a)).[12] To gain insight into the mechanism responsible for such transition, a comparison to a theoretical-atomistic model of the experiment was pursued (Fig. 2(b)). It was ascertained that measured yield stresses were consistent with a dislocation nucleation-controlled strain rate dependent model.[12, 20] The model includes an activation volume term, a quantity characterizing the governing thermally-activated dislocation mechanism.

Such activation volume can be computed numerically[12, 20] or experimentally. For the later, a MEMS consisting of two capacitive sensors on each side of the specimen, providing accurate measurements of stress and plastic strain, was successfully developed.[21-23] This MEMS device enables miniaturized transient tests such as repeated stress relaxation tests, and therefore simultaneous measurement of true activation volume and TEM observations of the governing mechanisms.

Investigation of coupled fields is another area in which MEMS devices find a natural application. Such coupled fields, e.g., piezo-resistivity and piezo-electricity, are of high relevance to emergent nanotechnologies based on low dimensional freestanding materials. It is known that when two-point measurements are performed, spurious size effects can results. Hence, novel micro-electro-mechanical systems that allow integrated four-point, uniaxial, electromechanical measurements of freestanding nanostructures in-situ electron microscopy, are needed. One implementation built on the thermal actuation-capacitive load measurement architecture.[24] Specifically, as is shown in Fig. 3 (a), four electrical traces coming from the outside electronics are connected by anchors and vias to very compliant, conductive folded beams that allow electrical access to the moving shuttles where the specimen is positioned. The folded beams are then interfaced with interconnects, which are brought to the vicinities of the specimen, Fig. 3 (b). The folded beams and interconnects are fabricated from highly-doped poly-silicon. In order to ensure that all four electrical signals are independent from each other, an insulating free-standing silicon nitride layer is deposited in the fabrication process. To complete the electrical connections to the specimen, Ion or Electron-Beam-Induced platinum deposition (IBID or EBID) is used to pattern connections from the poly-silicon interconnects to the specimen, Fig. 3(c). By employing such MEMS device, the piezo-resistivity of silver nanowires and n-type [111] silicon nanowires, up to unprecedented strain levels (>7%), was quantified, Fig. 3(d).[24]

In-Situ Fracture Tests

The first generation of MEMS mechanical test devices focused on extracting the uniaxial tensile stress-strain response of brittle thin films, allowing the determination of fracture stress σ_c, and the associated Weibull statistics.[25, 26] Combined with microscopy analysis, the σ_c distribution provides information on surface or bulk defects controlling cracking initiation and the inter- versus trans-granular propagation mechanisms for crystalline systems. Fracture toughness can be inferred from these tests based on the estimated defect size or vice versa.[27] Nevertheless, true fracture mechanics tests are preferable to more directly (and accurately) quantify fracture toughness, K_c. Hence, further developments aimed at testing pre-cracked fracture mechanics specimens with the interest to evaluate the fracture toughness as well as to stabilize the failure process and facilitate in-situ TEM analysis of the damage and fracture mechanisms.[28] In brittle films, the plastic zone size is in the nm scale which warrants valid K_c measurements. One difficulty is that extremely sharp pre-cracks are needed for valid measurements therefore caution should be taken with FIB precracking.[1] Precracking by crack arrest method is the most suitable approach.[29] Recently, a MEMS structure (see Fig. 4(a)) actuated by internal stress has been developed within a stable cracking configuration.[30] A crack is initiated from a notch, propagates and arrests due to a geometrically dictated decrease of K. The fracture toughness is determined from the final crack length after release of the test structure. The technique has been successfully applied to freestanding silicon nitride films. In-situ HRTEM analysis near the cleavage crack tip region under loading has the potential to provide new insights into the fundamental cracking mechanisms.

The fracture resistance of ductile films is quantified by the fracture strain ε_f, which is stress state dependent, or by K_c.[31] Fracture strain has been measured by MEMS test devices in a variety of ductile films.[32, 33] Similar to brittle films, the determination of K_c faces the problem of pre-cracking.[1] Crack arrest measurement from a notch using a MEMS structure is an option.[30] For these tests, K_c corresponds to the near plane stress regime and is thickness dependent.[34, 35] Nevertheless, the main merit of MEMS structures is to allow, on un-cracked or cracked specimens, in-situ TEM analysis on the evolution of plastic localization (see previous section), damage and near crack fracture process zone mechanisms under well controlled mechanical conditions.[36-38]

In-Situ Fatigue Tests

Characterizing nanoscale fatigue of metals is a critical research area, to provide a better understanding of small fatigue crack behavior as well as to ensure proper reliability of microcomponents. Metallic MEMS microresonators (Fig. 4(b)) are integrated fatigue testing machines, whereby a microbeam can be cycled at resonance under fully reversed loading conditions at large frequencies (kHz regime).[39-41] These devices are miniaturized versions of bulk ultrasonic fatigue testing, and as such, can be tested inside a SEM.[39] The evolution of the measured resonance frequency can be used as a proxy to quantify nanoscale fatigue damage including ultralow average crack growth rates.[39]

In-situ TEM nanodynamics is a powerful testing technique used in recent instruments to obtain fatigue properties and to observe structural changes during cyclic loading.[38, 42, 43] MEMS-based actuators, sensors, and sample mounts have been used to conduct high frequency in-situ fatigue tests. Bufford *et al.* recently studied tensile fatigue of nanocrystalline Cu film using a PTP MEMS-based sample mounting device.[43] PTP is an integrated MEMS device to apply tensile strain to one- and two-dimensional samples (*e.g.,* nanowires, nanotubes and thin films). The high resolution of the TEM enabled to observe structural changes and localized grain growth in front of the crack tip of Cu film. Using the captured crack growth video, a precise crack extension rate of 6×10^{-12} m·cycle^{-1} was calculated, which is equivalent to breaking tens of atomic bonds on average during each cycle.

In-Situ Wear Testing

Traditional tribology studies are limited by the inability to observe real-time progress of deformation at the sliding interfaces. Recent developments of small-scale devices, particularly piezoelectric and MEMS-based actuators, aid in observing atomic-scale dynamic deformation and understanding fundamentals of sliding contacts in single asperity wear, superlubricity, biomedical, and magnetic storage. MEMS actuators can provide high force- and displacement-resolution and good thermal stability which are important factors for obtaining precise mechanical properties and for capturing high resolution images during a tribology test. A "2D" MEMS transducer has been used recently in an in-situ cyclic nanofriction experiments on a single WS_2 nanoparticle.[44] Exfoliation of the particle during a sliding event was observed in the TEM which was correlated to the change in coefficient of friction. The transducer used in this study (Bruker Nano Surfaces, Minneapolis, USA) consists of two electrostatic micromachined comb drives in a single body that actuate and sense force and displacements in normal and lateral directions. A diamond tip was coupled to a comb drive that actuates a motion towards indentation axis and the second comb drive comprising a plurality of electrostatic capacitive actuators drives the same probe perpendicular to the indentation axis. This MEMS transducer was used in another study to understand failure mechanism of a perpendicular magnetic recording film stack under scratch loading.[45] The film structure consists of a 2 nm diamond-like carbon (DLC) protecting two functional layers below, which are a metallic layer and its stoichiometrically equivalent oxide. These types of films are widely utilized in storage devices and loss of data by grain reorientation in the recording layers is a primary failure mechanism. In-situ observation revealed that surface asperities on the DLC coating were removed at low normal force, where grain reorientation and debonding of the columnar metallic and oxide recording layers occurred at high normal force. A similar multi-cycle scratch test was run on Olivine specimen and the formation of dislocation plasticity was observed under the indenter tip (Fig. 5).[46] Symmetric arrays of defects appeared along the wear path and the number of arrays increased after each pass. The kinetic friction coefficient was determined as 0.1 and was relatively constant with numbers of wear passes. Recently, Sato *et al.* integrated two perpendicular MEMS actuators into a single device, then conducted in-situ wear tests using two silicon indenters attached to the actuators.[47] The interaction, deformation, and separation at the nanojunctions of silver nanoparticles were observed in the TEM while the normal and lateral forces were detected during the sliding event in real-time.

Outlook: Environmental In-Situ Nanomechanics

The above-mentioned in-situ nanomechanics techniques are currently mostly limited to vacuum conditions. While a few examples of MEMS in-situ techniques operating at high temperatures[9, 48] or under irradiation conditions exist,[49, 50] there is a clear need to extend MEMS platforms for nanomechanical testing beyond the high vacuum conditions within the TEM in order to study the structure-property relationship at the atomic-scale in technology relevant environments.[13] As such, integrating MEMS platforms with an ETEM[51] could be used to study the mechanical impact from redox environments, corrosive environments, hydrogen embrittlement, and catalytic reactions, all at variable gas compositions and temperatures. However, because the compatibility of the MEMS device with the ETEM imposes modifications to the functionality of the MEMS platform, the exposed regions of the MEMS platform and the electrical contacts must be evaluated for reactivity with the test gas to prevent adverse effects.[52] Though many studies have combined ETEM with quantitative straining holders,[53-55] demonstration of a nanomechanics MEMS platform within an ETEM has not been previously published.

Higher pressure gaseous and liquid experiments are generally conducted within the TEM using a hermetically sealed cell. These cells are composed of two silicon nitride (SiN) windows which confine the gaseous or liquid environment within, retaining atomic-scale imaging through constraint of the background scattering caused by the SiN window thickness and the gas/liquid thickness.[56] However, these have not yet been combined with mechanical actuation of the enclosed sample. A closed-cell Mechanical-Environmental-Thermal MEMS platform for tensile testing of electron transparent specimens within atmospheric gaseous or liquid environments is being developed,[57] which segregates the actuation elements from the static environmental cell using patterned barriers (see

Fig. 6). A barrier piston arm connects the sample (which is set between the SiN windows) to the actuator (which operates under an atmospheric environment). A hydrophobic self-assembled monolayer within the piston arm channel prevents liquid from leaking into the actuator. This platform has the potential to provide the lab-in-a-gap conditions needed to couple multiple modes of in-situ control (elevated temperature control and electrochemical contacts) to mechanical tensile testing within the TEM. For example, experiments on the mechanical properties of biological sub-micron materials may be conducted within this type of cell under physiologically relevant environmental conditions. Additionally, materials problems, such as stress-corrosion-cracking mechanisms and stress-induced electrochemical degradation mechanisms, can be visualized at the atomic-scale during operation of this MEMS device in a TEM.

Acknowledgments

This work (KJ and OP) was performed, in part, at the Center for Integrated Nanotechnologies, an Office of Science User Facility operated for the U.S. Department of Energy (DOE) Office of Science. Sandia National Laboratories is a multi-mission laboratory managed and operated by National Technology and Engineering Solutions of Sandia, LLC., a wholly owned subsidiary of Honeywell International, Inc., for the U.S. DOE's National Nuclear Security Administration under contract DE-NA-0003525. The views expressed in the article do not necessarily represent the views of the U.S. DOE or the United States Government. H.D.E. gratefully acknowledges support from NSF through awards No. DMR-1408901 and DMREF-CMMI-1235480, ARO through awards No. W911NF1510068 and MURI Award No. W911NF-08-1-054. OP acknowledges support of the NSF (awards DMR-1255046 and CMMI-1562499) and DOE-BES (DE-SC0018960).

Figure Captions

Figure 1. (a) MEMS fabricated on an SOI wafer.[16] (b) TEM image of single dislocation nucleation in penta-twinned silver nanowires.[11] (c) Dislocation glides back and disappears upon unloading (recoverable plasticity mechanism). Adapted with permission from NANO LETTERS. Copyright 2015 American Chemical Society.

Figure 2. (a) and (b) Brittle-to-ductile transition as a function of strain rate in silver nanowires.[12] Comparison of measured yield stress and molecular dynamic predictions via nucleation theory. Adapted with permission from NANO LETTERS. Copyright 2016 American Chemical Society

Figure 3. (a) MEMS for four-point electro-mechanical measurements. Scale bar 200 μm. (b) Image of shuttles in the specimen region and configuration of interconnects. Scale bar 40 μm. (c) Details of mounted specimen and traces of electron/ion beam induced deposition of platinum. Scale bar 4 μm. (d) Two- and four-point resistivity measurements as a function of strain for silver and silicon nanowires.[24] Reprinted with permission from SMALL. Copyright 2014 Wiley Co.

Figure 4. (a) MEMS-type fracture mechanics test: cracking is induced from a notch, the loading comes from internally stressed actuator beams and the fracture toughness is measured from the arrest crack length. (b) Top: SEM image of a Ni microresonator with an inclined magnification image of the microbeam. Bottom: Inclined SEM images of a microbeam after in-situ SEM fatigue test ($\sigma_a = 440$ MPa, fatigue life: 8.1×10^7 cycles). Adapted with permission from NANO LETTERS. Copyright 2018 American Chemical Society.[39]

Figure 5. (a) 2D MEMS load and displacement sensing transducer for in-situ tribological applications, (b) front part of a Hysitron in-situ nanomechanical instrument, TEM PicoIndenter showing location of the sample and transducer, and (c) Image montage showing gradual defect nucleation during 5 passes of an in-situ scratch test on single-crystal olivine.[46]

Figure 6. Mechanical-Environmental-Thermal MEMS platform for TEM testing of atmospheric gaseous or liquid environments with temperature control, electrochemical control, and displacement sensing capability. Lid (pink cross-section) and base (grey) are sealed using epoxy to create the static cell. Bond pads (copper) connect the MEMS device to the holder for external control.

Author biographies

Dr. Sanjit Bhowmick (9625 W 76th Street, Minneapolis, MN, sanjit.bhowmick@gmail.com, Tel: +1-952-835-6366; Fax: +1-952-835-6166) is a senior staff scientist at Bruker Nano, Inc. His research interests include *in situ* TEM and SEM characterization of mechanical properties of small-scale structures and high temperature properties of materials. He is involved in the development projects of nanomechanical instruments for electron microscopy (Hysitron's PicoIndenter products). He has authored or co-authored over 90 publications.

Horacio D. Espinosa (2145 Sheridan Rd., Evanston, IL 60208, 847-4675989, espinosa@nothwestern.edu) is the James and Nancy Farley Professor of Manufacturing and Entrepreneurship, Professor of Mechanical Engineering, and Director of the Theoretical and Applied Mechanics (TAM) Program at the McCormick School of Engineering and Applied Sciences at Northwestern University. He received his Ph.D. in Solid Mechanics from Brown University. Professor Espinosa has made contributions in the areas of dynamic failure of advanced materials, mechanics of biomaterials, and micro/nanomechanics. He is a foreign member of the European Academy of Arts and Sciences, the Russian Academy of Engineering, and *Fellow* of AAAS, AAM, ASME, and SEM. He received numerous awards and honors including the PRAGER medal from the Society of Engineering Science, the MURRAY and SIA NEMAT-NASSER medals from the Society for Experimental Mechanics (SEM), the ASME THURSTON award, and the LAZAN and HETENYI awards from SEM. He was the Timoshenko visiting Professor at Stanford University in 2011 and President of the Society of Engineering Science in 2012. Currently he serves in the U.S. National Committee on TAM and the IUTAM Congress Committee.

Katherine Jungjohann (P.O. Box 5800, Albuquerque, NM 87185-1304, 505-284-6892, 505-284-7778, kljungj@sandia.gov) is a staff scientist at the Center for Integrated Nanotechnologies (CINT) working on developing new capabilities for in-situ TEM imaging of environmentally relevant materials processes, with a current focus on energy storage interfaces and corrosion mechanisms. She is the thrust leader for the In-Situ Characterization and Nanomechanics Thrust at CINT and the co-leader of the Microscopy Society of America's Focused Interest Group on Electron Microscopy in Liquids and Gases.

Thomas Pardoen is full professor and President of the Institute of Mechanics, Materials and Civil Engineering at UCLouvain as well as chairman of the Scientific Council of the Belgian Nuclear Research Center SCK•CEN. He did his master in engineering, master in philosophy and PhD (1998) at UCLouvain, followed by a postdoctoral period at Harvard University. His research focuses on the nano-, micro- and macro- mechanics of materials with emphasis on multiscale experimental investigations and modelling of deformation and fracture. He has supervised 45 PhDs, 20 post docs, and published >200 papers in international journals. He received the 2011 Grand Prix Alcan of the French Academy of Sciences and a 2015 Francqui Chair, and was nominated Euromech Fellow 2015.

Olivier Pierron (801 Ferst Drive, Atlanta, GA 30332-0405, tel: +1 404-894-7877, olivier.pierron@me.gatech.edu) is a Professor in the Woodruff School of Mechanical Engineering at Georgia Tech. His research focuses on the mechanics of small-scale materials with emphasis on their degradation properties to assess and improve the reliability of devices and systems fabricated with emerging technologies. He is the recipient of the 2013 NSF CAREER Award and the 2014 Hetényi Award.

Figure 1

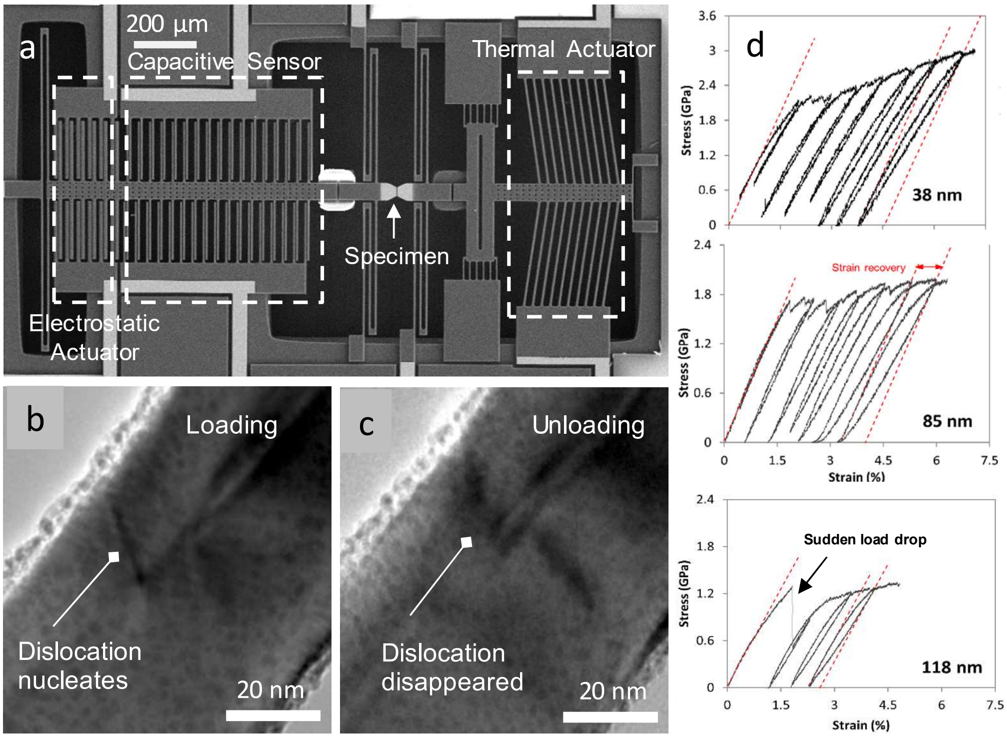
a
200 µm
Capacitive Sensor
Thermal Actuator
Specimen
Electrostatic Actuator
b
Loading
Dislocation nucleates
20 nm
c
Unloading
Dislocation disappeared
20 nm
d
Stress (GPa)
38 nm
Strain recovery
85 nm
Strain (%)
Sudden load drop
118 nm
Strain (%)

Figure 2

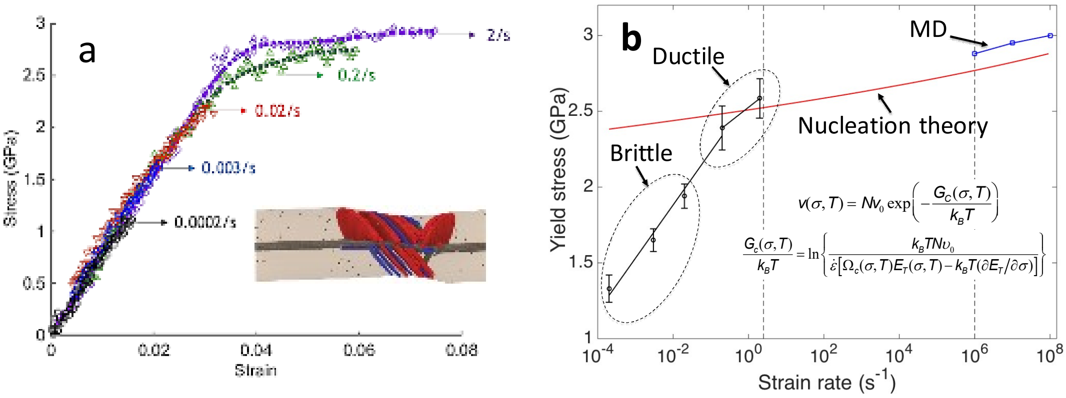

Figure 3

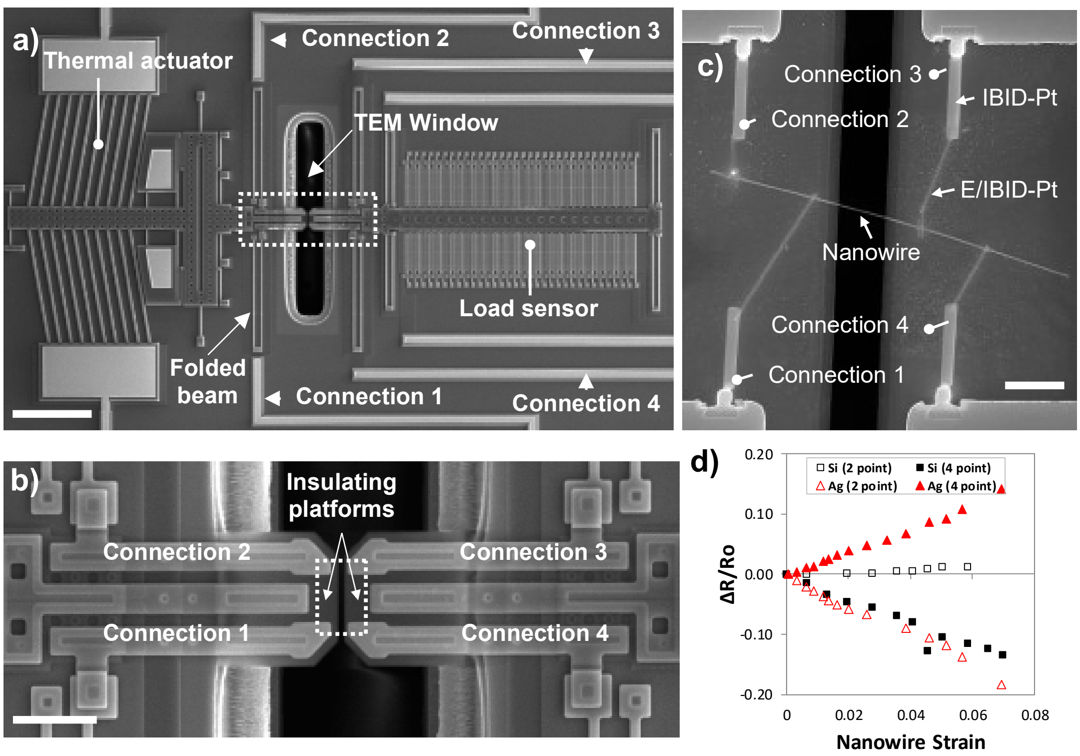

Figure 4

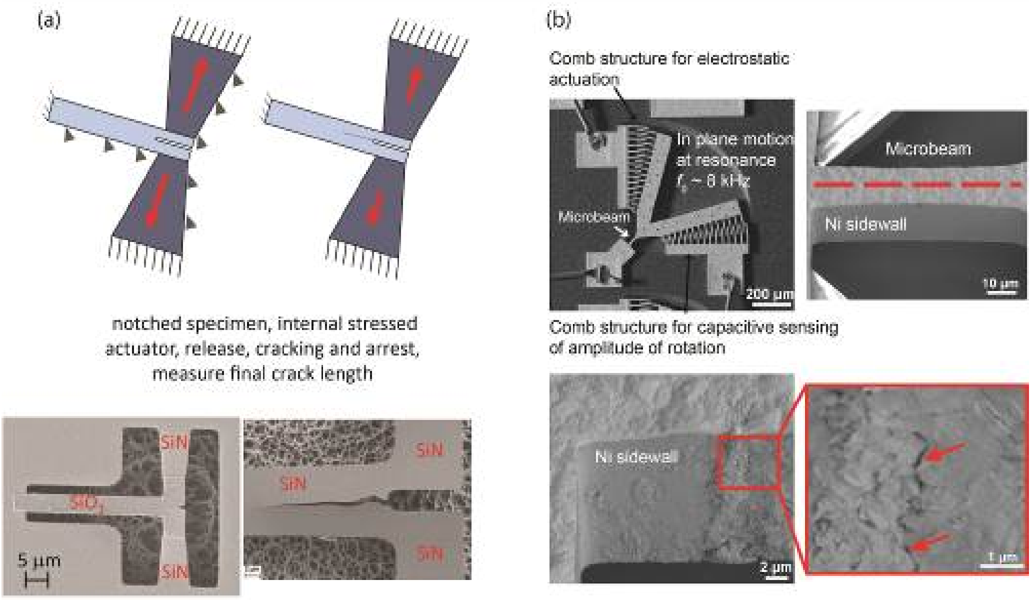

(a)
notched specimen, internal stressed actuator, release, cracking and arrest, measure final crack length
SiN
SiO2
5 μm
SiN
SiN
SiN
SiN
(b)
Comb structure for electrostatic actuation
In plane motion at resonance
f0 ~ 8 kHz
Microbeam
200 μm
Microbeam
Ni sidewall
10 μm
Comb structure for capacitive sensing of amplitude of rotation
Ni sidewall
2 μm
1 μm

Figure 5

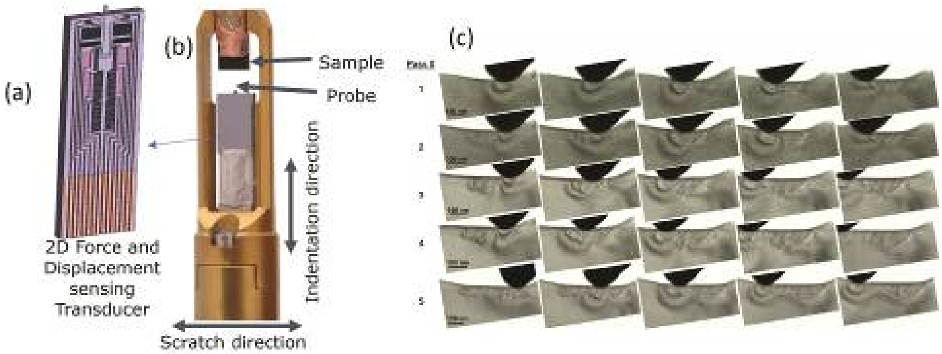

Figure 6

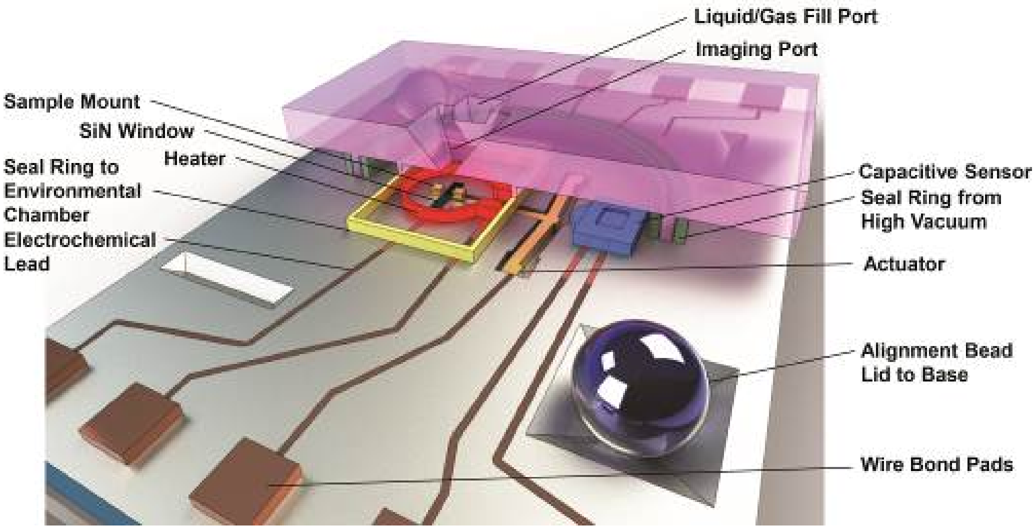

1. G. Dehm, B. N. Jaya, R. Raghavan, C. Kirchlechner, *Acta Materialia* **142**, 248-282 (2018).
2. H. D. Espinosa, R. A. Bernal, T. Filleter, *Small* **8**, 3233-3252 (2012).
3. M. A. Haque, H. D. Espinosa, H. J. Lee, *MRS Bulletin* **35**, 375-381 (2010).
4. M. J. Hytch, A. M. Minor, *Mrs Bulletin* **39**, 138-146 (2014).
5. M. Legros, *Comptes Rendus Physique* **15**, 224-240 (2014).
6. M. Legros, D. S. Gianola, C. Motz, *MRS Bulletin* **35**, 354-360 (2010).
7. R. Ramachandramoorthy, R. Bernal, H. D. Espinosa, *ACS Nano* **9**, 4675-4685 (2015).
8. Q. Yu, M. Legros, A. M. Minor, *Mrs Bulletin* **40**, 62-68 (2015).
9. Y. Zhu, T. H. Chang, *J. Micromech. Microeng.* **25**, 21 (2015).
10. J. Kacher, T. Zhu, O. N. Pierron, D. Spearot, *COSSMS* **under review**, (2019).
11. R. A. Bernal *et al.*, *Nano Letters* **15**, 139-146 (2015).
12. R. Ramachandramoorthy, W. Gao, R. Bernal, H. Espinosa, *Nano Letters* **16**, 255-263 (2016).
13. R. Ramachandramoorthy *et al.*, *ACS Nano* **11**, 4768-4776 (2017).
14. T. Filleter, R. Bernal, S. Li, H. D. Espinosa, *Adv. Mater.* **23**, 2855-+ (2011).
15. B. Peng *et al.*, *Nat. Nanotechnol.* **3**, 626-631 (2008).
16. M. F. Pantano, R. A. Bernal, L. Pagnotta, H. D. Espinosa, *Meccanica* **50**, 549-560 (2015).
17. R. Bernal, Ramachandramoorthy, R., Espinosa, H.D., *Ultramicroscopy* **156**, 23-28 (2015).
18. T. Sannicolo, Lagrange,M., Cabos, A., Celle, C., Simonato, J.P., Bellet, D.,, *Small* **12**, 6052-6075 (2016).
19. R. Ramachandramoorthy *et al.*, *Extreme Mechanics Letters* **20**, 14-20 (2018).
20. T. Zhu, Li, J., Samanta, A., Leach, A., Gall, K., *Physical Review Letters* **100**, 025502 (2008).
21. E. Hosseinian, M. Legros, O. N. Pierron, *Nanoscale* **8**, 9234-9244 (2016).
22. S. Gupta, O. Pierron, *J. Microelectromech. Sys.* **26**, 1082-1092 (2017).
23. S. Gupta, O. N. Pierron, *Extreme Mechanics Letters* **8**, 167-176 (2016).
24. R. A. Bernal *et al.*, *Small* **10**, 725-733 (2014).
25. A. van der Rest *et al.*, *Acta Materialia* **125**, 27-37 (2017).
26. V. Passi *et al.*, *J. Microelectromech. Sys.* **21**, 822-829 (2012).
27. S. Yagnamurthy, B. L. Boyce, I. Chasiotis, *J. Microelectromech. Sys.* **24**, 1436-1452 (2015).
28. P. Zhang *et al.*, *Nat. Commun.* **5**, 7 (2014).
29. V. Hatty, H. Kahn, A. H. Heuer, *J. Microelectromech. Sys.* **17**, 943-947 (2008).
30. S. Jaddi, M. Coulombier, J. P. Raskin, T. Pardoen, *J. Mech. Phys. Sol.* **123**, 267-291 (2019).
31. A. Pineau, A. Amine Benzerga, T. Pardoen, *Acta Materialia*.
32. M. P. de Boer *et al.*, *Acta Materialia* **56**, 3313-3326 (2008).

33. K. Jonnalagadda, N. Karanjgaokar, I. Chasiotis, J. Chee, D. Peroulis, *Acta Materialia* **58**, 4674-4684 (2010).
34. H. Hosokawa, A. V. Desai, M. A. Haque, *Thin Solid Films* **516**, 6444-6447 (2008).
35. W. R. Lanning, S. S. Javaid, C. L. Muhlstein, *Fatigue and Fracture of Engineering Materials and Structures* **40**, 1809-1824 (2017).
36. F. Mompiou *et al.*, *Acta Materialia* **61**, 205-216 (2013).
37. E. Hosseinian, S. Gupta, O. N. Pierron, M. Legros, *Acta Materialia* **143**, 77-87 (2018).
38. S. Kumar, M. T. Alam, M. A. Haque, *J. Microelectromech. Sys.* **20**, 53-58 (2011).
39. A. Barrios, S. Gupta, G. M. Castelluccio, O. N. Pierron, *Nano Letters* **18**, 2595-2602 (2018).
40. F. Sadeghi-Tohidi, O. N. Pierron, *Acta Materialia* **106**, 388-400 (2016).
41. F. Sadeghi-Tohidi, O. N. Pierron, *Extreme Mechanics Letters* **9**, 97-107 (2016).
42. E. Hosseinian, O. Pierron, *Nanoscale* **5**, 12532-12541 (2013).
43. D. C. Bufford *et al.*, *Nano Letters* **16**, 4946-4953 (2016).
44. I. Z. Jenei, F. Dassenoy, *Tribology Letters* **65**, 8 (2017).
45. E. D. Hintsala, D. D. Stauffer, Y. Oh, S. A. S. Asif, *Jom* **69**, 51-56 (2017).
46. S. Bhowmick, E. Hintsala, D. Stauffer, S. A. S. Asif, *Microsc. microanal.* **24**, 1934-1935 (2018).
47. T. Sato, E. Tochigi, T. Mizoguchi, Y. Ikuhara, H. Fujita, *Microelectronic Engineering* **164**, 43-47 (2016).
48. M. Elhebeary, M. T. A. Saif, *Extreme Mechanics Letters* **23**, 1-8 (2018).
49. P. Lapouge *et al.*, *Acta Materialia* **131**, 77-87 (2017).
50. P. Lapouge *et al.*, *Journal of Nuclear Materials* **476**, 20-29 (2016).
51. E. D. Boyes, P. L. Gai, *Comptes Rendus Physique* **15**, 200-213 (2014).
52. D. S. Gianola *et al.*, *Review of Scientific Instruments* **82**, 063901 (2011).
53. T. Epicier *et al.*, in *European Microscopy Congress 2016: Proceedings*. (Wiley Online Library, 2016), pp. 145-146.
54. P. Ferreira, I. Robertson, H. Birnbaum, *Acta materialia* **46**, 1749-1757 (1998).
55. D. Xie *et al.*, *Nat. Commun.* **7**, 13341 (2016).
56. K. Jungjohann, C. B. Carter, in *Transmission Electron Microscopy*. (Springer, 2016), pp. 17-80.
57. K. L. Jungjohann *et al.* (Google Patents, 2018).